

than well-folded substrates (see Supplementary Information). This permitted the development of a gel-based assay that used susceptibility to deglycosylation as an indicator of the entropic state of gp120, either alone or in complex with an antibody.

Deglycosylation

Deglycosylations were performed with gp120 produced in *Drosophila* Schneider 2 lines. Carbohydrate analysis of this protein showed that about 70% of the attached sugars were sensitive to digestion by endoglycosidase H (Endo H), the rest being a smaller (mannose)₃ variety. The gp120 proteins included core + V3 loop from both YU2 and JRFL, and full-length HXBc2. Mass-spectroscopy analysis of full-length HXBc2 before and after digestion by Endo H showed relative molecular masses of 84,200 ± 2,600 and 64,000 ± 1,600, respectively.

Deglycosylation reactions were performed in 350 mM NaCl under a variety of different conditions with pH varying between 5.5 and 6.5, reaction times between 2 and 20 h, and gp120 concentrations between 0.1 and 1.0 mg ml⁻¹. Reactions were generally performed at 37 °C; reducing the temperature to 20 °C altered the slope of the normalization but not the degree of fit. Ligands were added to a minimum ligand-binding-site:gp120 stoichiometry of 1.5:1 to ensure the complete binding of all gp120. Ligands were CD4 (domains 1 and 2), purified monoclonal antibodies, or antigen-binding portions of antibodies.

Results from five separate deglycosylation experiments are reported here, two with full-length HXBc2, two with YU2 (core + V3 loop) and one with JRFL (core + V3 loop). In each of these experiments, 5–10 different ligands were tested, of which at least half had entropies determined by isothermal titration calorimetry and could be used for calibration. The ligand make-up and relative rates of deglycosylation for each experiment are given in the Supplementary Information.

Sequencing

Sequencing of 17b and 48d antibodies was accomplished with primers that encoded the N termini of the variable domains and the conserved constant-region hinge sequences. Sequences and methodology are detailed in the Supplementary Information.

Neutralization

D1D2-IgGtp was made as described previously²¹. Neutralization assays were performed on freshly isolated activated peripheral-blood mononuclear cells as described²⁶. Activated cells (200,000) were inoculated with 100 tissue-culture-infectious-dose-50 units of each isolate, with the simultaneous addition of sCD4, D1D2-IgGtp or PBS. Virus was washed from the cells after 24 h. Cultures were maintained for 15 days in the presence of interleukin-2-containing medium. Reverse-transcriptase activity was measured on a day before peak replication in the control supernatants. All cultures were performed in quintuplicate.

Received 28 May; accepted 23 September 2002; doi:10.1038/nature01188.

- Weiss, R. A. *et al.* Neutralization of human T-lymphotropic virus type III by sera of AIDS and AIDS-risk patients. *Nature* **316**, 69–72 (1985).
- Kwong, P. D. *et al.* Structure of an HIV gp120 envelope glycoprotein in complex with the CD4 receptor and a neutralizing human antibody. *Nature* **393**, 648–659 (1998).
- Myszka, D. G. *et al.* Energetics of the HIV gp120-CD4 binding reaction. *Proc. Natl Acad. Sci. USA* **97**, 9026–9031 (2000).
- Dalgleish, A. G. *et al.* The CD4 (T4) antigen is an essential component of the receptor for the AIDS retrovirus. *Nature* **312**, 763–767 (1984).
- Feng, F., Broder, C. C., Kennedy, P. E. & Berger, E. A. HIV-1 entry co-factor: functional cDNA cloning of a seven-transmembrane, G protein-coupled receptor. *Science* **272**, 872–877 (1996).
- Klatzmann, D. *et al.* T-lymphocyte T4 molecule behaves as the receptor for human retrovirus LAV. *Nature* **312**, 767–768 (1984).
- Posner, M. R. *et al.* An IgG human monoclonal antibody that reacts with HIV-1/GP120, inhibits virus binding to cells, and neutralizes infection. *J. Immunol.* **146**, 4325–4332 (1991).
- Thali, M. *et al.* Characterization of conserved human immunodeficiency virus type 1 (HIV-1) gp120 neutralization epitopes exposed upon gp120-CD4 binding. *J. Virol.* **67**, 3978–3988 (1993).
- Burton, D. R. *et al.* Efficient neutralization of primary isolates of HIV-1 by a recombinant human monoclonal antibody. *Science* **266**, 1024–1027 (1994).
- Moore, J. P. & Sodroski, J. Antibody cross-competition analysis of the human immunodeficiency virus type 1 exterior envelope glycoprotein. *J. Virol.* **70**, 1863–1872 (1996).
- Trkola, A. *et al.* Human monoclonal antibody 2G12 defines a distinctive neutralization epitope on the gp120 glycoprotein of human immunodeficiency virus type 1. *J. Virol.* **70**, 1100–1108 (1996).
- Rizzuto, C. D. *et al.* A conserved human immunodeficiency virus gp120 glycoprotein structure involved in chemokine receptor binding. *Science* **280**, 1949–1953 (1998).
- Binley, J. M. *et al.* Analysis of the interaction of antibodies with a conserved, enzymatically deglycosylated core of the HIV-1 gp120 envelope glycoprotein. *AIDS Res. Hum. Retroviruses* **14**, 191–198 (1998).
- Sites, W. E. Protein-protein interactions: interface structure, binding thermodynamics, and mutational analysis. *Chem. Rev.* **97**, 1233–1250 (1997).
- Kwong, P. D. *et al.* Structures of HIV-1 gp120 envelope glycoproteins from laboratory-adapted and primary isolates. *Structure* **8**, 1329–1339 (2000).
- Luque, I. & Freire, E. A system for the structure-based prediction of binding affinities and molecular design of peptide ligands. *Methods Enzymol.* **295**, 100–127 (1998).
- Fouts, T. R., Binley, J. M., Trkola, A., Robinson, J. E. & Moore, J. P. Neutralization of the human immunodeficiency virus type 1 primary isolate JR-FL by human monoclonal antibodies correlates with antibody binding to the oligomeric form of the envelope glycoprotein complex. *J. Virol.* **71**, 2779–2785 (1997).
- Sullivan, N. *et al.* CD4-induced conformational changes in the human immunodeficiency virus type 1 gp120 glycoprotein: consequences for virus entry and neutralization. *J. Virol.* **72**, 4694–4703 (1998).
- Salzwedel, K., Smith, E. D., Dey, B. & Berger, E. A. Sequential CD4-coreceptor interactions in human immunodeficiency virus type 1 env function: soluble CD4 activates env for co-receptor-dependent fusion and reveals blocking activities of antibodies against cryptic conserved epitopes on gp120. *J. Virol.* **74**, 326–333 (2000).

- Moore, J. P., McKeating, J. A., Huang, Y. X., Ashkenazi, A. & Ho, D. D. Virions of primary human immunodeficiency virus type 1 isolates resistant to soluble CD4 (sCD4) neutralization differ in sCD4 binding and glycoprotein gp120 retention from sCD4-sensitive isolates. *J. Virol.* **66**, 235–243 (1992).
- Arthos, J. *et al.* Biochemical and biological characterization of a dodecameric CD4-Ig fusion protein. Implications for therapeutic and vaccine strategies. *J. Biol. Chem.* **277**, 11456–11464 (2002).
- Zhu, P., Olson, W. C. & Roux, K. H. Structural flexibility and functional valence of CD4-IgG2 (PRO 542): Potential for cross-linking human immunodeficiency type 1 envelope spikes. *J. Virol.* **75**, 6682–6686 (2001).
- Trauneker, A., Schneider, J., Kiefer, H. & Karjalainen, K. Highly efficient neutralization of HIV with recombinant CD4-immunoglobulin molecule. *Nature* **339**, 68–70 (1989).
- Wyatt, R. *et al.* The antigenic structure of the human immunodeficiency virus gp120 envelope glycoprotein. *Nature* **393**, 705–711 (1998).
- Doyle, M. L. *et al.* Measurement of protein interaction bioenergetics: application to structural variants of anti-sCD4 antibody. *Methods Enzymol.* **323**, 207–230 (2000).
- Zhou, J. Y. & Montefiori, D. C. Antibody-mediated neutralization of primary isolates of human immunodeficiency virus type 1 in peripheral blood mononuclear cells is not affected by the initial activation state of the cells. *J. Virol.* **71**, 2512–2517 (1997).
- Kwong, P. D., Wyatt, R., Sattentau, Q. J., Sodroski, J. & Hendrickson, W. A. Oligomeric modeling and electrostatic analysis of the gp120 envelope glycoprotein of the human immunodeficiency virus. *J. Virol.* **74**, 1961–1972 (2000).
- Wyatt, R. *et al.* Analysis of the interaction of the human immunodeficiency virus type 1 gp120 envelope glycoprotein with the gp41 transmembrane glycoprotein. *J. Virol.* **71**, 9722–9731 (1997).
- Fung, M. S. *et al.* Identification and characterization of a neutralization site within the second variable region of human immunodeficiency virus type 1 gp120. *J. Virol.* **66**, 848–856 (1992).
- Rusche, J. R. *et al.* Antibodies that inhibit fusion of human immunodeficiency virus-infected cells bind a 24-amino acid sequence of the viral envelope, gp120. *Proc. Natl Acad. Sci. USA* **85**, 3198–3202 (1988).

Supplementary Information accompanies the paper on Nature's website (<http://www.nature.com/nature>).

Acknowledgements We thank M. Dybul for providing primary isolates pi102, pi104, pi202 and pi204; M. A. Gawinowicz for matrix-assisted laser desorption/ionization-time of flight analysis; Z. Moodie and A. Palmer for help with error analysis; A. Fauci, S. Harrison, A. Miranker, R. Seder and L. Shapiro for discussions; and D. Dimitrov, B. Kwong, N. Letvin, J. Mascola, G. Nabel and Q. Sattentau for comments. This work was supported by grants from the National Institutes of Health and by a Center for AIDS Research grant to the Dana-Farber Cancer Institute. The Dana-Farber Cancer Institute is also the recipient of a Cancer Center Grant from the National Institutes of Health. Columbia University is a participant in a Center for AIDS Research. R.W. was a fellow of the American Foundation for AIDS Research and P.D.K. was a recipient of a Burroughs Wellcome Career Development award.

Competing interests statement The authors declare that they have no competing financial interests.

Correspondence and requests for materials should be addressed to P.D.K. (e-mail: pdkwong@nih.gov).

Asymmetric inheritance of centrosomally localized mRNAs during embryonic cleavages

J. David Lambert* & Lisa M. Nagy

Department of Molecular and Cellular Biology, University of Arizona, Tucson, Arizona 85721, USA

During development, different cell fates are generated by cell-cell interactions or by the asymmetric distribution of patterning molecules. Asymmetric inheritance is known to occur either through directed transport along actin microfilaments into one daughter cell^{1,2} or through capture of determinants by a region of the cortex inherited by one daughter^{3–5}. Here we report a third mechanism of asymmetric inheritance in a mollusc embryo. Different messenger RNAs associate with centrosomes in different cells and are subsequently distributed asymmetrically during division. The segregated mRNAs are diffusely distributed in the cytoplasm and then localize, in a microtubule-dependent

* Present address: Department of Genetics, Yale University School of Medicine, New Haven, Connecticut 06520, USA.

manner, to the pericentriolar matrix. During division, they dissociate from the core mitotic centrosome and move by means of actin filaments to the presumptive animal daughter cell cortex. In experimental cells with two interphase centrosomes, mRNAs accumulate on the correct centrosome, indicating that differences between centrosomes control mRNA targeting. Blocking the accumulation of mRNAs on the centrosome shows that this event is required for subsequent cortical localization. These events produce a complex pattern of mRNA localization, in which different messages distinguish groups of cells with the same birth order rank and similar developmental potentials.

During embryonic cleavage cycles in molluscs and related proto-stome phyla, most of the early cell divisions are asymmetric, producing cells that differ in size, subsequent cleavage pattern and eventual fate (Fig. 1). Embryological experiments implicate both cell lineage and cell signalling in the establishment of embryonic cell fates in molluscs^{6–9}. While examining the roles of conserved developmental patterning genes in the mollusc *Ilyanassa obsoleta*, we found that mRNAs for several patterning genes show marked changes in subcellular localization during cleavage stages. Here we focus on three such genes: *IoEve*, which encodes a protein involved in anterior–posterior axis specification in other organisms¹⁰; *IoDpp*, the orthologue of *dpp* (or bone morphogenetic protein 2 (*BMP2*) and *BMP4* in vertebrates), which encodes a secreted signalling molecule^{11,12}; and *IoTld*, which encodes a secreted protease that is predicted to be a modifier of Dpp signalling¹³. *IoDpp* and *IoTld* have a role in specifying head precursor cells after the 24-cell stage (our unpublished data) and *IoEve* seems to be involved in patterning a subset of cells along the animal–vegetal axis of the embryo. We have focused on the events that position these mRNAs during early cleavage cycles.

The mRNAs were localized to the centrosome during the early cleavage cycles, and this localization led to asymmetric inheritance during cleavage (Fig. 2). In the four-cell stage, *IoEve* mRNA was found in all four cells on a spherical structure that lies between the nucleus and the animal pole of the embryo (Fig. 2g). Similarly, at the

eight-cell stage, *IoDpp* mRNA was localized to a spherical structure located anticlockwise to the nucleus in all four of the macromere cells (Fig. 2a). These mRNA-binding structures were at the centre of the microtubule arrays in these cells and were rich in γ -tubulin and centrin (Fig. 2be). We therefore conclude that these mRNA-binding structures are the interphase centrosomes.

Comparisons of γ -tubulin, β -tubulin and centrin staining with the distribution of mRNA suggested that the mRNA is bound throughout the pericentriolar matrix (PCM). Transmission electron micrographs confirmed that a zone of PCM occupies a region of the size predicted from other markers (Fig. 2f), showing that the mRNA

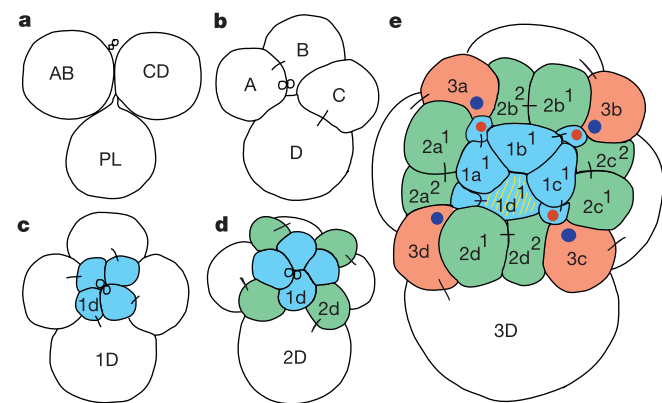


Figure 1 Diagram of *Ilyanassa* cleavage and patterns of centrosomally localized mRNA. **a, b**, The first two divisions are unequal and are accompanied by the production of a polar lobe (PL) at the vegetal pole, which results in a four-cell stage with one large and three smaller cells. These cells (macromeres) are the founder cells of the four lineages of the embryo, the A, B, C and D quadrants. **c–e**, In successive cleavage cycles, the macromeres function as stem cells, producing a stereotyped series of smaller cells towards the animal pole (micromeres). The four micromere cells produced by the macromeres in a given cleavage cycle are called a quartet. Quartet members have similar cleavage patterns and cell fates that differ from those of other quartets. This suggests that each quartet of micromeres receives similar patterning cues, although the mechanism is not known. The first quartet (1a–d) is blue (**c**), the second (2a–d) is green (**d**), and the third (3a–d) is orange (**e**). A summary of the patterns of centrosomally localized mRNAs described here (see Fig. 4) at the 24-cell stage is shown in **e**. *IoTld* is yellow, *IoEve* is red, and *IoDpp* is dark blue. Sister cells from the previous division are connected by a dash.

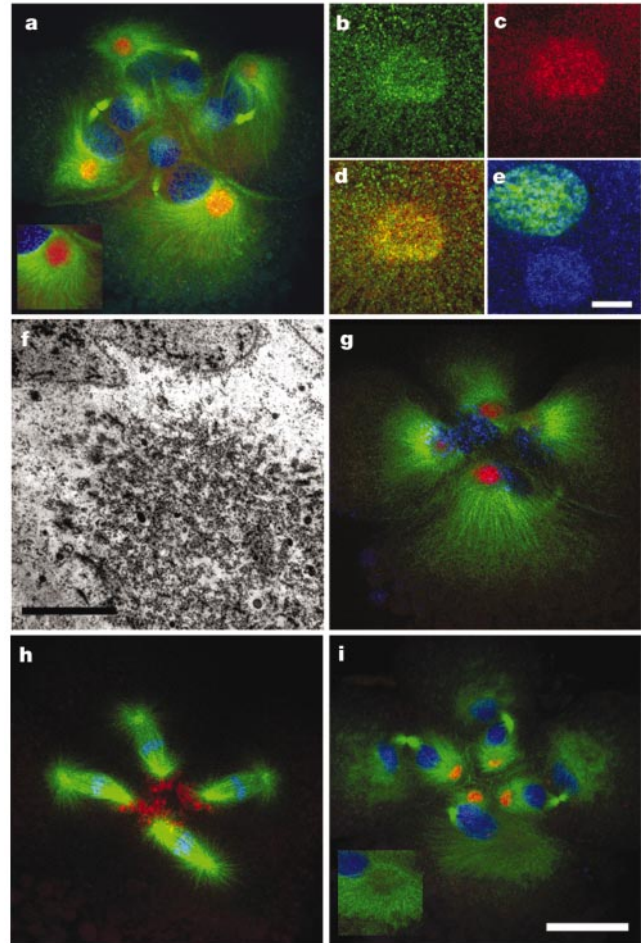


Figure 2 Localization of mRNAs to the centrosome and mRNA dynamics during cleavage. **a**, *In situ* hybridization with *IoDpp* mRNA to an eight-cell interphase embryo. The midbodies of the previous division are visible clockwise from each macromere nucleus (projection of confocal *z* series); inset, single section through the 1D centrosome (see Fig. 1b). **b–d**, γ -Tubulin (**b**) is bound to the same spherical structure as the *IoDpp* mRNA (**c**); merged in **d**. **e**, Centrin is enriched on a spherical structure located anticlockwise and vegetal to the macromere nuclei. **f**, Transmission electron micrograph of 1D nucleus (top left) and centrosome shows typical PCM composition of the size predicted by other markers. **g**, *In situ* hybridization with *IoEve* mRNA during early prophase of the four-cell stage (single confocal section, B and D macromere centrosomes in the plane of focus). **h, i**, *In situ* hybridization with *IoEve* mRNA during pro-metaphase at the transition to the eight-cell stage (**h**; projection) and in an early eight-cell embryo (**i**; projection). Inset, single section through the centrosome in 1D shows that *IoEve* is not present on this centrosome. mRNAs were visualized by HNPP/Fast Red precipitate (red; **a, c, d, g–i**), nuclei by DAPI (blue; **a, g–i**) or YOYO-1 (green; **e**), β -tubulin and γ -tubulin antibodies by Alexafluor-488-conjugated secondary antibodies (green; **a, b, d, g–i**), and monoclonal 20H5 antibodies^{26,27} against centrin with Cy5-conjugated secondary antibodies (blue; **e**). Animal views of the 1D centrosome are shown in **b–f**; animal views of whole embryos are shown in **a, g–i**. Scale bars, 5 μ m (**f**); 10 μ m (**e**); 50 μ m (**i**).

is localized throughout the PCM of the centrosome. By contrast, the distribution of the mRNA of a gene that is not predicted to be involved in patterning, the 40S ribosomal subunit, was distributed diffusely throughout the cytoplasm of all cells and not localized to centrosomes (data not shown).

The centrosomally localized mRNAs were partitioned into one daughter cell during division. For example, during prophase of the third cleavage, the *IoEve* mRNA moved to the granules in the region of the cortex of each macromere that was closest to the animal pole (Fig. 2h). At the same time, two small prophase asters were first detected in place of the large interphase centrosome, and these migrated into position for mitosis. During division, the cortically localized mRNA was segregated solely into the animal daughter cell, such that after cell division, the mRNA was present only on the centrosome in this cell (Fig. 2i). This movement between the interphase centrosome and the presumptive micromere cortex in mitosis was observed with all patterning mRNAs studied (see also Fig. 3b, c).

All of the centrosome-localized mRNAs that we examined showed these two discrete types of intracellular movement: an initial recruitment to particular interphase centrosomes, followed by a movement to a cortical region that would be inherited exclusively by one daughter cell in a given division. We investigated the cytoskeletal requirements of the observed mRNA movement by treating embryos with agents that specifically disrupt the cytoskeleton (Fig. 3). At the four-cell stage, *IoDpp* mRNA was distributed diffusely in the cytoplasm (Fig. 3a). During cytokinesis at the transition to the eight-cell stage, it became localized specifically to the centrosomes in macromeres, but not in micromeres (which are their sister cells), and the mRNA remained on the centrosomes during interphase (Fig. 3b). During prophase of the fourth division, the mRNA moved to a portion of the cortex that would be inherited by the second quartet cells (Fig. 3c).

Depolymerization of microtubules with nocodazole when *IoDpp* mRNA was still spread throughout the cytoplasm left most of the mRNA distributed diffusely in the cytoplasm, with some mRNA in disorganized filamentous structures (Fig. 3d). This was not due to a secondary loss of mRNA from the centrosome, because other

experiments showed that nocodazole treatment after localization had occurred did not disrupt the interphase pattern. Disrupting microfilament polymerization with cytochalasin B over the same time period did not prevent accumulation of mRNA on the centrosome (data not shown and Fig. 4f). Thus, an intact microtubule cytoskeleton is required for accumulation of mRNA on the centrosome.

We next investigated the basis of the movement of centrosome-bound mRNAs to the cortex during prophase. Inhibiting microtubule polymerization with nocodazole did not prevent movement of the mRNA (data not shown). But when actin filaments were induced to depolymerize with cytochalasin B just before and during the movement to the cortex, the mRNA remained near the nucleus and did not migrate to the cortex (Fig. 3e). Cytochalasin B treatment after the mRNA had moved to the cortex did not release

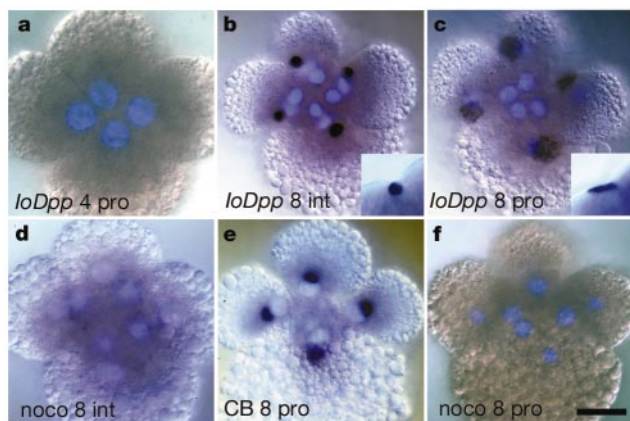


Figure 3 Cytoskeletal basis of mRNA localization. **a–c**, *In situ* hybridization with *IoDpp* mRNA at interphase of the four-cell stage (**a**), interphase of the eight-cell stage (**b**) and prophase of the eight-cell stage (**c**). Insets, lateral view of the 1D macromere centrosome (**b**); lateral view of *IoDpp* on the animal cortex of 1D (**c**). **d**, Embryo fixed 30 min after treatment with nocodazole (noco) during cytokinesis at the transition to eight-cell stage, when *IoDpp* mRNA was still spread around the cytoplasm (as in **a**). *IoDpp* mRNA was localized to the centrosome in controls (**b**). **e**, Treatment with cytochalasin B (CB) during interphase at the eight-cell stage, before *IoDpp* mRNA had moved to the cortex (compare with end-point control; **c**). **f**, Embryo treated with nocodazole as described in **d**, but fixed later during pro-metaphase. mRNAs are visualized by alkaline phosphatase precipitate (blue/black), nuclei by DAPI (light blue). Scale bar, 50 μ m.

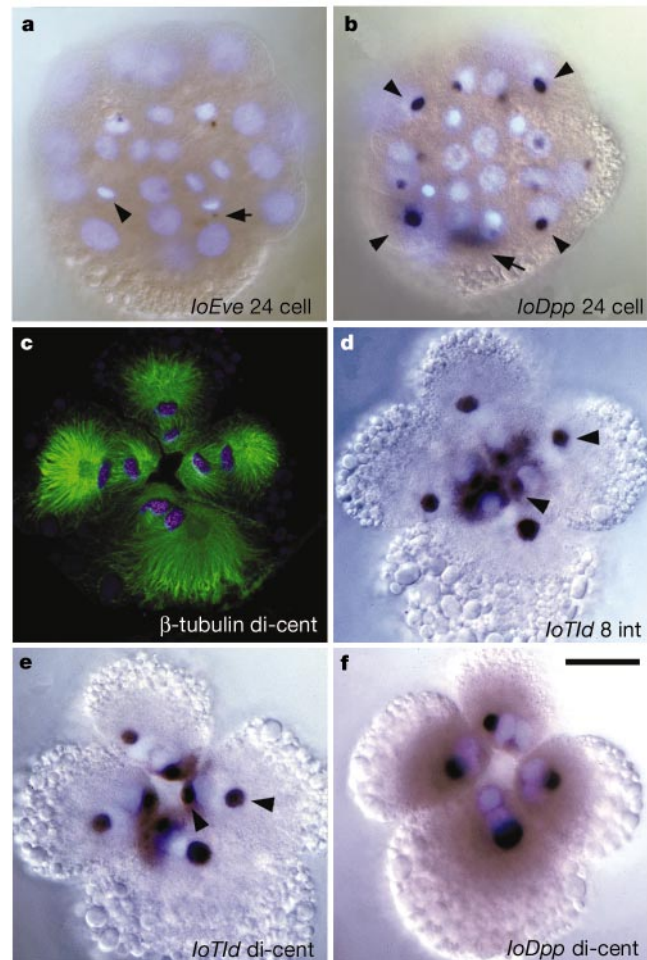


Figure 4 mRNAs are localized to specific subsets of cells during cleavage, and mRNAs are specifically targeted to particular centrosomes. **a**, *In situ* hybridization with *IoEve* mRNA at the 24-cell stage (arrow indicates $1c^2$, arrowhead indicates $1d^2$). **b**, *In situ* hybridization with *IoDpp* mRNA at the 24-cell stage. *IoDpp* is abundant on the centrosomes in 3a–d (arrowheads) and in a cloud above the nucleus of the 3D macromere (arrow). These patterns of localization are illustrated in Fig. 1e. **c, f, g**, Treatment with cytochalasin B during cytokinesis at the third cleavage cycle generates di-centrosomal embryos. **c**, Two microtubule-organizing centres (β -tubulin staining, green) and two nuclei (DAPI staining, blue) are seen in each of the four cells in cytochalasin-B-treated embryos (single confocal section). **d**, *In situ* hybridization with *IoTid* in a normal eight-cell embryo (arrowheads indicate centrosomes in the cells 1c and 1C). **e**, *In situ* hybridization with *IoTid* in di-centrosomal embryos. Arrowheads indicate the pair of centrosomes in the single C quadrant cell. **f**, *In situ* hybridization with *IoDpp* in di-centrosomal embryos. mRNAs are visualized by alkaline phosphatase precipitate (blue/black), nuclei by DAPI (light blue). Scale bar, 50 μ m.

the mRNA (data not shown). Thus, actin filaments, but not intact microtubules, are required for attraction or docking at the cell periphery. We therefore propose that mRNAs that require segregation for their subsequent roles in embryonic patterning are loaded onto the centrosome by minus-end-directed transport along microtubules. This movement prepares them for their subsequent delivery by actin filaments to a region of the cell cortex that will be inherited by a particular daughter cell.

We next considered whether accumulation on the cortex would occur without previous localization to the centrosome. We blocked *IoDpp* mRNA accumulation on the centrosome (as shown in Fig. 3d) and examined *IoDpp* mRNA at the onset of mitosis, a stage when mRNA is localized on the cortex in control embryos. We did not observe any cortical *IoDpp* mRNA staining (Fig. 3f). This was not a consequence of arrest or delay after treatment, because the chromosomal arrangement and condensation indicated that macromere nuclei were in prophase and pro-metaphase as in control embryos, and also *IoDpp* mRNA was not cortically localized at later time points. Because nocodazole treatment after localization to the centrosome does not affect centrosomal localization or movement to the cortex, this result indicates that mRNA movement to the cortex requires its previous accumulation on the centrosome.

We followed *IoEve*, *IoDpp* and *IoTld* in later cleavages stages. All three were associated with centrosomes, and all three were sorted during cell division (Fig. 4a, b). By the 24-cell stage, *IoEve* became localized to three particular cells that give rise to the ciliated band of the larvae (the primary trochoblasts 1a–c²; Fig. 4a). *IoDpp* was segregated into the second and third quartet micromeres, but decayed in the second quartet cells after the production of the third quartet, resulting in a specific localization in the third quartet cells, as well as in one macromere (the '3D' cell; Fig. 4b). *IoTld* was loaded onto centrosomes in all of the first quartet cells, but persisted only in the dorsal cell 1d¹ (data not shown). These patterns of mRNA distribution show that several patterning genes are localized specifically to certain subsets of cells by centrosome-mediated sorting. In addition, the subsets of micromere cells that contain a given mRNA have the same birth order rank and have similar cell fates and cleavage patterns^{14–16}. Our results suggest that these groups may be distinguished by centrosome-mediated segregation of patterning molecules.

The patterns of mRNA accumulation on the centrosomes of different cells suggest that intrinsic differences between these centrosomes control message accumulation. To test this, we produced diploid cells that contained two interphase centrosomes by blocking cytokinesis at the transition to the eight-cell stage with cytochalasin B (Fig. 4c–f). *IoTld* mRNA, which was present on centrosomes of both the animal and vegetal daughter cells in controls, was present on both centrosomes in di-centrosomal cells (Fig. 4d, e), showing that in these cells the two centrosomes lie at predictable locations that correspond to the locations of the centrosomes in the two normal daughter cells. *IoDpp* mRNA, which was on only the vegetal daughter centrosomes in controls (Fig. 3b), was found on only vegetal centrosomes in di-centrosomal cells (Fig. 4f). Thus, mRNAs are specifically targeted to certain centrosomes, so that even within the same cytoplasm a message accumulates on the correct centrosome. This suggests that intrinsic differences between centrosomes result in accumulation of particular mRNAs on centrosomes in certain cells. Because localization to the centrosome is required for subsequent cortical localization and segregation, differences in mRNA recruitment between centrosomes could thus control the segregation of mRNAs in the next cleavage cycle.

The mechanisms of asymmetric inheritance of patterning molecules have been investigated in several other systems^{2–4}. In *I. obsoleta*, as in other systems such as the *Drosophila melanogaster* neuroblast divisions, segregated molecules bind to a particular region of the cortex before division^{3,5}. But the role that we describe

for the centrosome during asymmetric cell division—that is, the site where segregated mRNAs are localized before moving to the cortex—has not been reported. Although the prior localization of these molecules to the centrosome has not been described, it is apparently not unusual in this system: we observed it with several different mRNAs and in successive cleavage cycles. It may represent a general mechanism of embryonic patterning in this embryo. The role that we show for the centrosome is reminiscent of mechanisms of asymmetric cell division from other systems. In ascidians, regions of the cortex that bind localized mRNAs interact with centrosomes during asymmetric cell division^{17,18}. In the *Caenorhabditis elegans* embryo, degradation of PIE-1 protein on the anterior centrosome of P1 complements other mechanisms to segregate the protein to the posterior daughter^{19,20}. Our observations provide a link between the segregation of determinants and the cleavage apparatus in asymmetric cell divisions. Centrosomes replicate at each cell cycle in somatic cells, and the daughter centrosomes are generally considered to be equivalent. But evidence suggests that there can be functional differences between the two centrosomes in a dividing cell^{21–23}. Our work indicates that cells can exploit differences between centrosomes in different cells to target patterning molecules for asymmetric partitioning during division.

E. G. Conklin²⁴, working with the mollusc *Crepidula* in 1902, described a distinct portion of cytoplasm that surrounded the core mitotic centrosome during interphase in the macromeres. This structure moved to the cortex before division and was inherited in its entirety by the micromeres. He called this structure the 'sphere', to distinguish it from the core mitotic centrosome. Our results corroborate Conklin's observations and show that the sphere is a part of the interphase centrosome, and that it contains mRNAs for several developmental patterning genes. These results suggest that, during early cleavages in mollusc embryos, the centrosome is the site of assembly for a package of molecules that is then delivered to one daughter cell, and that this mechanism distinguishes sets of equivalent cells during cleavage. This mechanism may operate in other systems where a stem cell produces a stereotyped series of daughter cells with different fates. □

Methods

RNA *in situ* hybridization and immunohistochemistry

Fragments of complementary DNAs were cloned by polymerase chain reaction (PCR) with degenerate primers, followed by rapid amplification of cDNA ends with PCR to obtain larger fragments for *in situ* hybridization. For colocalization of mRNAs and the microtubule skeleton cytoskeleton, and for most standard *in situ* hybridizations, we fixed embryos in PEM (100 mM PIPES, pH 6.9, 10 mM EGTA and 1 mM MgSO₄) with 8% paraformaldehyde, 100 mM sucrose and 0.1% Triton X-100. For the *in situ* hybridizations shown in Fig. 4a, b, embryos were fixed in 3.7% formalin in 90% filtered artificial sea water. For all *in situ* hybridizations, embryos were pretreated for 10 min in 2% acetic anhydride in TEA buffer and prehybridized for 3 h at 63 °C in Hyb solution (5 × SSC, 1 × Denhart's, 50% formamide, 1% Tween 20, 100 µg ml⁻¹ heparin and 100 µg ml⁻¹ yeast rRNA plus tRNA), hybridized with 1–10 ng ml⁻¹ digoxigenin-labelled probe for 12–18 h, washed three times over 2 h with Hyb solution at 63 °C. Non-fluorescent *in-situ* were detected by nitro blue tetrazolium/5-bromo-4-chloro-3-indolyl phosphate precipitation. For colocalization with the microtubule cytoskeleton, samples were incubated at 23 °C overnight with monoclonal mouse antibodies against β-tubulin (Developmental Studies Hybridoma Bank) plus antibodies against digoxigenin conjugated to alkaline phosphatase. Alkaline phosphatase detection of hybridized probes was carried out with HNPP/Fast Red substrate (Boehringer-Mannheim) as described²⁵, followed by overnight incubation at 23 °C with secondary antibodies against mouse IgG. We carried out γ-tubulin staining with a rabbit polyclonal antibody generated against an epitope found in human γ-tubulin (Sigma). Centrin staining was done with two mouse monoclonals (20H5 and 11B2) generated against the *Chlamydomonas reinhardtii* centrin protein, both of which recognize centrin in animal cells^{26,27}. Animal maintenance, embryo collection, antibody staining, YOYO-1 (Molecular probes) and 4',6-diamidino-2-phenylindole dihydrochloride (DAPI) staining and all other steps were done as described²⁸.

Transmission electron microscopy

Embryos were fixed for 3–6 h in 2% glutaraldehyde and 95% artificial sea water, and then postfixed in 2% OsO₄ for 1–2 h.

Inhibitor experiments

We made solutions of the inhibitors in dimethyl sulphoxide at 1,000 times the final concentrations. Nocodazole was used at 1 µg ml⁻¹ (Fig. 3d) or 10 µg ml⁻¹ (in all other

nocodazole assays); both concentrations were sufficient to block cleavage and depolymerize essentially all microtubules, as judged by staining with antibodies against β -tubulin. We used cytochalasin B at $20 \mu\text{g ml}^{-1}$, a concentration sufficient to block cleavage and to depolymerize essentially all actin filaments, as judged by phalloidin staining.

Received 12 February; accepted 10 October 2002; doi:10.1038/nature01241.

1. Takizawa, P. A., Sil, A., Swedlow, J. R., Herskowitz, I. & Vale, R. D. Actin-dependent localization of an RNA encoding a cell-fate determinant in yeast. *Nature* **389**, 90–93 (1997).
2. Long, R. M. *et al.* Mating type switching in yeast controlled by asymmetric localization of ASH1 mRNA. *Science* **277**, 383–387 (1997).
3. Spana, E. P. & Doe, C. Q. The Prospero transcription factor is asymmetrically localized to the cell cortex during neuroblast mitosis in *Drosophila*. *Development* **121**, 3187–3195 (1995).
4. Boyd, L., Guo, S., Levitan, D., Stinchcomb, D. T. & Kemphues, K. J. PAR-2 is asymmetrically distributed and promotes association of P granules and PAR-1 with the cortex in *C. elegans* embryos. *Development* **122**, 3075–3084 (1996).
5. Lu, B. W., Ackerman, L., Jan, L. Y. & Jan, Y. N. Modes of protein movement that lead to the asymmetric localization of partner of numb during *Drosophila* neuroblast division. *Mol. Cell* **4**, 883–891 (1999).
6. Crampton, H. E. Experimental studies on gastropod development. *Roux's Arch. EntwMech. Org.* **3**, 1–19 (1896).
7. Clement, A. C. Experimental studies on germinal localization in *Ilyanassa*. I. The role of the polar lobe in determination of the cleavage pattern and its influence in later development. *J. Exp. Zool.* **132**, 427–446 (1952).
8. Wilson, E. B. Experimental studies in germinal localization. II Experiments on the cleavage-mosaic in patella and dentalium. *J. Exp. Zool.* **1**, 197–268 (1904).
9. Clement, A. C. Development of *Ilyanassa* following the removal of the D macromere at successive cleavage stages. *J. Exp. Zool.* **149**, 193–216 (1962).
10. Macdonald, P. M., Ingham, P. & Struhl, G. Isolation, structure, and expression of *even-skipped*—a 2nd pair-rule gene of *Drosophila* containing a homeo box. *Cell* **47**, 721–734 (1986).
11. Wharton, K. A., Ray, R. P. & Gelbart, W. M. An activity gradient of Decapentaplegic is necessary for the specification of dorsal pattern elements in the *Drosophila* embryo. *Development* **117**, 807–822 (1993).
12. Holley, S. A. *et al.* A conserved system for dorsal–ventral patterning in insects and vertebrates involving Sog and Chordin. *Nature* **376**, 249–253 (1995).
13. Shimell, M. J., Ferguson, E. L., Childs, S. R. & O'Connor, M. B. The *Drosophila* dorsal–ventral patterning gene *Tollid* is related to human bone morphogenetic protein-1. *Cell* **67**, 469–481 (1991).
14. Clement, A. C. Cell determination and organogenesis in molluscan development—reappraisal based on deletion experiments in *Ilyanassa*. *Am. Zool.* **16**, 447–453 (1976).
15. Render, J. Cell fate maps in the *Ilyanassa obsoleta* embryo beyond the third division. *Dev. Biol.* **189**, 301–310 (1997).
16. Sweet, H. C. Specification of first quartet micromeres in *Ilyanassa* involves inherited factors and position with respect to the inducing D macromere. *Development* **125**, 4033–4044 (1998).
17. Yoshida, S., Marikawa, Y. & Satoh, N. posterior end mark, a novel maternal gene encoding a localized factor in the ascidian embryo. *Development* **122**, 2005–2012 (1996).
18. Nishikata, T., Hibino, T. & Nishida, H. The centrosome-attracting body, microtubule system, and posterior egg cytoplasm are involved in positioning of cleavage planes in the ascidian embryo. *Dev. Biol.* **209**, 72–85 (1999).
19. Mello, C. C. *et al.* The PIE-1 protein and germline specification in *C. elegans* embryos. *Nature* **382**, 710–712 (1996).
20. Reese, K. J., Dunn, M. A., Waddle, J. A. & Seydoux, G. Asymmetric segregation of PIE-1 in *C. elegans* is mediated by two complementary mechanisms that act through separate PIE-1 protein domains. *Mol. Cell* **6**, 445–455 (2000).
21. Wu, X. Y. & Palazzo, R. E. Differential regulation of maternal vs. paternal centrosomes. *Proc. Natl Acad. Sci. USA* **96**, 1397–1402 (1999).
22. Bonaccorsi, S., Giansanti, M. G. & Gatti, M. Spindle assembly in *Drosophila* neuroblasts and ganglion mother cells. *Nature Cell Biol.* **2**, 54–56 (2000).
23. Piel, M., Meyer, P., Khodjakov, A., Rieder, C. L. & Bornens, M. The respective contributions of the mother and daughter centrioles to centrosome activity and behavior in vertebrate cells. *J. Cell Biol.* **149**, 317–329 (2000).
24. Conklin, E. G. Karyokinesis and cytokinesis in the maturation, fertilization and cleavage of *Crepidula* and other gastropoda. *J. Acad. Nat. Sci. Philadelphia Ser.* **2** **12**, 1–21 (1902).
25. Goto, S. & Hayashi, S. Cell migration within the embryonic limb primordium of *Drosophila* as revealed by a novel fluorescence method to visualize mRNA and protein. *Dev. Genes Evol.* **207**, 194–198 (1997).
26. Sanders, M. A. & Salisbury, J. L. Centrin plays an essential role in microtubule severing during flagellar excision in *Chlamydomonas reinhardtii*. *J. Cell Biol.* **124**, 795–805 (1994).
27. Paoletti, A., Moudjou, M., Paintrand, M., Salisbury, J. L. & Bornens, M. Most of centrin in animal cells is not centrosome-associated and centrosomal centrin is confined to the distal lumen of centrioles. *J. Cell Sci.* **109**, 3089–3102 (1996).
28. Lambert, J. D. & Nagy, L. M. MAPK signaling by the D quadrant embryonic organizer of the mollusc *Ilyanassa obsoleta*. *Development* **128**, 45–56 (2001).

Acknowledgements We thank J. Cooley, D. Bentley and J. Wandelt for technical help; J. Salisbury and G. Hermann for antibodies; D. Brower, C. Gregorio and G. Von Dassow for critically reading the manuscript; and R. Palazzo, M. Goulding, G. Lambert, E. Wilk and M. Gibson for technical advice and discussions. This work was supported by an National Science Foundation (NSF) Graduate Research Fellowship and an NSF Doctoral Dissertation Improvement Grant to J.D.L., and a grant from the NSF to L.M.N.

Competing interests statement The authors declare that they have no competing financial interests.

Correspondence and requests for materials should be addressed to L.M.N. (e-mail: lnagy@u.arizona.edu). Sequences have been deposited in GenBank under accession codes AF499914 (*IoDpp*), AF499912 (*IoEve*), AF499913 (*IoTld*) and AY151152 (*Io40S*).

Endocytosis-mediated downregulation of LIN-12/Notch upon Ras activation in *Caenorhabditis elegans*

Daniel D. Shaye* & Iva Greenwald†‡

* Departments of Genetics and Development and † Biochemistry and Molecular Biophysics, and ‡ Howard Hughes Medical Institute, Columbia University, College of Physicians and Surgeons, New York, New York 10032, USA

The coordination of signals from different pathways is important for cell fate specification during animal development. Here, we define a novel mode of crosstalk between the epidermal growth factor receptor/Ras/mitogen-activated protein kinase cascade and the LIN-12/Notch pathway during *Caenorhabditis elegans* vulval development. Six vulval precursor cells (VPCs) are initially equivalent but adopt different fates as a result of an inductive signal mediated by the Ras pathway and a lateral signal mediated by the LIN-12/Notch pathway¹. One consequence of activating Ras is a reduction of LIN-12 protein in P6.p (ref. 2), the VPC believed to be the source of the lateral signal. Here we identify a 'downregulation targeting signal' (DTS) in the LIN-12 intracellular domain, which encompasses a di-leucine-containing endocytic sorting motif. The DTS seems to be required for internalization of LIN-12, and on Ras activation it might mediate altered endocytic routing of LIN-12, leading to downregulation. We also show that if LIN-12 is stabilized in P6.p, lateral signalling is compromised, indicating that LIN-12 downregulation is important in the appropriate specification of cell fates *in vivo*.

The six VPCs, consecutively numbered P3.p–P8.p, have the potential to adopt one of three fates, 1°, 2° or 3°, which can be distinguished by cell lineage and marker gene expression (see Fig. 1). In wild-type hermaphrodites, P3.p–P8.p always adopt the same pattern of fates (3°, 3°, 2°, 1°, 2° and 3°, respectively) as a result of inductive and lateral signalling events (reviewed in ref. 1). The inductive signal, LIN-3, produced by the anchor cell of the gonad activates the receptor tyrosine kinase LET-23 and a canonical Ras/mitogen-activated protein kinase (MAPK) cascade in P6.p to promote the 1° fate. An unknown lateral signal, believed to be produced by P6.p, activates LIN-12 in P5.p and P7.p to promote the 2° fate. Loss of SUR-2, a Ras target that is a component of the Mediator transcription factor complex³, abrogates lateral signalling⁴; thus Ras activation might control the transcription of the lateral signal and/or of factors required to activate this signal.

Ras activation also causes downregulation of a LIN-12::green-fluorescent-protein (GFP) reporter in P6.p and its descendants². However, a *lin-12::lacZ* transcriptional reporter is expressed continuously in the VPCs and their daughters⁵, suggesting that transcriptional control of *lin-12* is not the mechanism by which downregulation of LIN-12 is accomplished, in contrast to another paradigmatic LIN-12-mediated cell fate decision in *C. elegans*⁶. Here we explore two related issues, the mechanism of post-transcriptional downregulation of LIN-12 in response to Ras activation, and the role of this downregulation in VPC fate specification.

We hypothesized that there would be a DTS within LIN-12. To identify this signal, we used the *egl-17* promoter (*egl-17p*), which is activated in P6.p in response to the inductive signal⁷, to express GFP-tagged LIN-12 fragments in P6.p and its descendants. Extra-chromosomal arrays carrying such constructs were marked with *egl-17p::LacZ*, and transgenic hermaphrodites were stained with anti-GFP and anti-LacZ antibodies at the time of vulval induction (see Methods). LacZ will be expressed in P6.p and its daughters after